J|A|C|S
ARTICLES
Published on Web 01/21/2003

Probing the Dynamic Guest−Host Interactions in Sol−Gel Films Using Single Molecule Spectroscopy

C. Ricardo Viteri,[†] James W. Gilliland,[‡] and Wai Tak Yip*,[‡]

Contribution from the Universidad San Francisco de Quito, Apartado 17-12-841, Quito, Ecuador and Department of Chemistry and Biochemistry, University of Oklahoma, Norman, Oklahoma 73019

Received April 15, 2002; E-mail: ivan-yip@ou.edu

Abstract: Organic dyes usually exhibit enhanced photostability when trapped inside sol−gel silicates. The enhanced photostability is attributed to the reduction of intramolecular motions that facilitate photodegradation. We report the simultaneous detection of mobility and photostability of sol−gel encapsulated didodecyl-3,3,3′,3′-tetramethylindocarbocyanine (DiI) using single molecule spectroscopy. Fluorescence from DiI was resolved into parallel and perpendicular polarization components and separately detected. On the basis of the calculated fluorescence polarization, single DiI molecules were classified into "tumbling" and "fixed". Out of 212 molecules investigated, 52% were found to be fixed. For the first time, the mobility of a guest molecule in sol−gel silicate can be directly correlated with its own photostability. Both tumbling and fixed molecules have shown to exhibit nonuniform photostability, indicative of the very heterogeneous guest−host interactions within each subgroup. The survival lifetimes for the majority of the tumbling and fixed molecules were found to be 4.3 and 13.1 s, respectively, demonstrating unequivocally that fixed molecules exhibit a higher photostability than tumbling molecules. These results are in accordance with a recent study on rhodamine B encapsulated in dried sol−gel silicates.

Introduction

The sol−gel process is a low temperature synthetic technique for the preparation of inorganic oxides. The synthesis is usually carried out at room temperature using metal alkoxide as a starting material.[1] One of the most widely used starting materials is tetralkyl orthosilicate ($Si(OR)_4$), from which sol−gel silicate can be made. Scheme 1 illustrates the two reactions that best describe the sol−gel process. In the presence of water, silicon alkoxide first hydrolyzes into silanol, which then subsequently polycondensates with one another randomly into a porous and disorganized three-dimensional framework of silicon oxide. During the polycondensation process, many silanol groups will remain unreacted and distribute randomly throughout the entire sol−gel framework. Hence, sol−gel silicate is a porous material that is both structurally and chemically heterogeneous.

The porous nature of the sol−gel framework provides two distinctive advantages that are critical to the widespread application of sol−gel derived materials. First, it allows the trapping of many guest molecules introduced either before or after the polycondensation reaction. Indeed, the incorporation of organic dyes into porous silicate hosts using the sol−gel method has provided a valuable alternative to designing new optical materials. The preparation of dye-doped sol−gel composites is highly flexible, and the choice of inorganic substrate (host) and dye dopant (guest) is almost unlimited. If the host and guest are chosen properly, it is possible to tailor new photonic materials with desirable optical properties.[2] For examples, dye-doped silicate monoliths have been utilized in the fabrication of many solid-state devices including dye laser systems,[3−7] optical waveguide arrays,[8] and other photochromic materials.[9] Second, even though a guest molecule is well retained inside a sol−gel matrix, it can still interact with many external reagents that are small enough to diffuse through the porous framework. This second merit leads to the development of a wide array of chemical and biological sensors using sol−gel derived materials.[10] For examples, a pH sensing device can be constructed from a fluorescein-doped silica sol−gel matrix,[11] the spectral response of pyranine encapsulated inside a sol−gel silicate can be used to estimate the aqueous content in a

Scheme 1. Sol−Gel Process

$$Si(OR)_4 + nH_2O \xrightarrow{\text{hydrolysis}} Si(OR)_{4-n}(OH)_n + nROH$$

$$\equiv Si\text{-}OH + HO\text{-}Si\equiv \xrightarrow[\text{condensation}]{\text{poly-}} \equiv Si\text{-}O\text{-}Si\equiv + H_2O$$

[†] Universidad San Francisco de Quito.
[‡] University of Oklahoma.

(1) Brinker, C. J.; Scherer, G. *Sol−Gel Science, The Physics and Chemistry of Sol−Gel Processing*; Academic Press: San Diego, CA, 1989.
(2) Reisfeld, R. *Opt. Mater.* **2001**, *16*, 1−7.
(3) McKiernan, J. M.; Yamanaka, S. A.; Dunn, B.; Zink, J. I. *J. Phys. Chem.* **1990**, *94*, 5652−5654.
(4) McKiernan, J. M.; Yamanaka, S. A.; Knobbe, E.; Pouxviel, J.; Parvanch, S.; Dunn, B.; Zink, J. I. *J. Inorg. Organomet. Polym.* **1991**, *1*, 87−103.
(5) Knobbe, E. T.; Dunn, B.; Fuqua, P. D.; Nishida, F.; Zink, J. I. In *Ultrastructure Processing of Advanced Materials*; Uhlmann, D. R., Ulrich, D. R., Eds.; John Wiley & Sons: New York, 1992; pp 519−529.
(6) Reisfeld, R.; Yariv, E.; Minti, H. *Opt. Mater.* **1997**, *8*, 31−36.
(7) Yariv, E.; Reisfeld, R. *Opt. Mater.* **1999**, *13*, 49−54.
(8) Yang, P. D.; Wirnsberger, G.; Huang, H. C.; Cordero, S. R.; McGehee, M. D.; Scott, B.; Deng, T.; Whitesides, G. M.; Chmelka, B. F.; Buratto, S. K.; Stucky, G. D. *Science* **2000**, *287*, 465−467.
(9) Levy, D. *Chem. Mater.* **1997**, *9*, 2666−2670.
(10) Liang, L. F.; Li, Y. T.; Yang, V. C. *J. Pharm. Sci.* **2000**, *89*, 979−990.
(11) Villegas, M. A.; Pascual, L. *J. Mater. Sci.* **2000**, *35*, 4615−4619.

10.1021/ja026533k CCC: $25.00

Scheme 2. Route to Photodegradation of a Dye Molecule

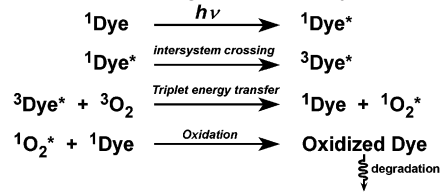

solution mixture,[12] the concentration of hydrogen peroxide can be accurately determined by measuring the chemiluminescence produced by a sol−gel encapsulated horseradish peroxidase biocomposite,[13] and glucose concentration can be routinely monitored by a glucose oxidase-doped silica sol−gel matrix.[14]

The rational design of solid-state photonic materials with desirable optical properties rests on our understanding of the interactions between an encapsulated molecule and its immediate surroundings. Accordingly, the study of optical properties of dye-doped solid hosts has been a subject of intense research.[11,15−24] There is increasing evidence to suggest that when an organic dye is trapped inside a sol−gel silicate, it exhibits a higher photostability.[15,25−28] The enhanced photostability of organic dyes found in a silica sol−gel host is arguably due to two major factors. The first one is the caging effect of the host on the dye molecules. When trapped inside a cavity of a physically comparable dimension, a dye molecule will experience hindered intramolecular motions. This reduction in intramolecular freedom is believed to enhance photostability by reducing the number of dynamic interactions that favor photodegradation. The second factor is reduced photo-oxidation. As illustrated by the series of reactions outlined in Scheme 2, photo-oxidation provides a major route to the destruction of an organic dye molecule. After a singlet excited dye molecule relaxes to a triplet state via intersystem crossing, it can easily transfer the excitation energy to a nearby oxygen molecule and produce a highly reactive singlet oxygen species ($^1\Delta_g$). This highly energetic oxygen molecule will then oxidize the dye nearby and lead to photodegradation of the dye molecule.[29−32] In particular, photo-oxidation occurs frequently inside a solvent host in which oxygen can diffuse freely toward a dye molecule. On the contrary, the densely networked environment inside a sol−gel silicate is believed to slow the diffusion of oxygen substantially, thereby minimizing photodegradation.[29,31]

It is worthwhile to point out that the postulation which suggests that hindered intramolecular motions will improve photostability is actually inferred from many different ensemble measurements.[7,22,33,34] However, a molecular property obtained from ensemble measurements is at best a statistical average of the observable. It is therefore almost impossible to interpret the relationship between different molecular properties measured from separate experiments. This is especially true in the case when dye molecules are trapped inside silica sol−gel films, where the pore size, pore shape, and the chemical environment between different pores are highly heterogeneous.[35] In other words, every encapsulated dye molecule is surrounded by a very different microenvironment. Hence, it remains uncertain if there really is a direct correlation between the intramolecular motions and photostability of a guest molecule encapsulated inside a sol−gel silicate host. As pointed out by Dunn et al., sol−gel encapsulated guest molecules generally reside in four different environments: (i) the interior of pores that are filled with liquid; (ii) the solid−liquid interface; (iii) the solid pore wall; and (iv) the constraining cleft region that extends deep into the pore wall.[24] As a result, a molecule trapped in different local environments is expected to display a different photophysical behavior.[36] Evidently, to better understand the origin of improved photostability of organic dyes encapsulated inside a silica sol−gel matrix, it is necessary to monitor the mobility and photostability of the dye molecules at the single molecule level.

Single molecule spectroscopy is an exciting new area of research. It aims at studying the physical and optical properties of individual molecules and thereby completely eliminates the statistical effect inherent to ensemble measurements. Recent advances in solid-state technology have allowed the optical detection of single molecules at room temperature.[37] The application of single molecule spectroscopy in both physical and biological sciences has been reviewed recently.[37−41] In this project, we will employ single molecule spectroscopy to study organic dyes trapped inside a silica sol−gel film in order to gain molecular-level insight into the caging effect on the optical properties of an encapsulated molecule. Of particular interest is how the mobility of a molecule relates to its own photostability. The successful application of sol−gel silicate derived photonic materials relies critically on the photostability of the dye dopants, which are highly sensitive to the nature of their

(12) Wasiucionek, M.; Breiter, M. W. *J. Non-Cryst. Solids* **1997**, *220*, 52−57.
(13) Diaz, A. N.; Peinado, M. C. R.; Minguez, M. C. T. *Anal. Chim. Acta* **1998**, *363*, 221−227.
(14) Wu, X. J.; Choi, M. M. F.; Xiao, D. *Analyst* **1999**, *125*, 157−162.
(15) Avnir, D.; Levy, D.; Reisfeld, R. *J. Phys. Chem.* **1984**, *88*, 5956−5959.
(16) Suratwala, T.; Gardlund, Z.; Davidson, K.; Uhlmann, D. R.; Bonilla, S.; Peyghambarian, N. *J. Sol-Gel Sci. Technol.* **1997**, *8*, 973−978.
(17) Suratwala, T.; Gardlund, Z.; Davidson, K.; Uhlmann, D. R.; Watson, J.; Bonilla, S.; Peyghambarian, N. *Chem. Mater.* **1998**, *10*, 199−209.
(18) Suratwala, T.; Gardlund, Z.; Davidson, K.; Uhlmann, D. R.; Watson, J.; Peyghambarian, N. *Chem. Mater.* **1998**, *10*, 190−198.
(19) Yariv, E.; Schultheiss, S.; Saraidarov, T.; Reisfeld, R. *Opt. Mater.* **2001**, *16*, 29−38.
(20) Takahashi, Y.; Maeda, A.; Kojima, K.; Uchida, K. *J. Lumin.* **2000**, *87*−*9*, 767−769.
(21) Perez-Bueno, J. J.; Diaz-Flores, L. L.; Perez-Robles, J. F.; Espinoza-Beltran, F. J.; Ramirez-Bon, R.; Vorobiev, Y. V.; Gonzalez-Hernandez, J. *Microelectron. Eng.* **2000**, *51*−*2*, 667−675.
(22) Casalboni, M.; Dematteis, F.; Francini, R.; Prosposito, P.; Senesi, R.; Grassano, U. M.; Pizzoferrato, R.; Gnappi, G.; Montenero, A. *J. Lumin.* **1997**, *72*−*4*, 475−477.
(23) De Matteis, F.; Prosposito, P.; Sarcinelli, F.; Casalboni, M.; Pizzoferrato, R.; Furlani, A.; Russo, M. V.; Vannucci, A.; Varasi, M. *J. Non-Cryst. Solids* **1999**, *245*, 15−19.
(24) Dunn, B.; Zink, J. I. *Chem. Mater.* **1997**, *9*, 2280−2291.
(25) Dubois, A.; Canva, M.; Brun, A.; Chaput, F.; Boilot, J. P. *Synth. Met.* **1996**, *81*, 305−308.
(26) Yagi, K.; Shibata, S.; Yano, T.; Yasumori, A.; Yamane, M.; Dunn, B. *J. Sol-Gel Sci. Technol.* **1995**, *4*, 67−73.
(27) Nishida, F.; Dunn, B.; McKiernan, J. M.; Zink, J. I.; Brinker, C. J.; Hurd, A. J. *J. Sol-Gel Sci. Technol.* **1994**, *2*, 477−81.
(28) Nishida, F.; McKiernan, J. M.; Dunn, B.; Zink, J. I.; Brinker, C. J.; Hurd, A. J. *J. Am. Ceram. Soc.* **1995**, *78*, 1640−1648.
(29) Rahn, M. D.; King, T. A.; Gorman, A. A.; Hamblett, I. *Appl. Opt.* **1997**, *36*, 5862−5871.
(30) Panzer, O.; Gohde, W.; Fischer, U. C.; Fuchs, H.; Mullen, K. *Adv. Mater.* **1998**, *10*, 1469−1472.
(31) Ahmad, M.; Rahn, M. D.; King, T. A. *Appl. Opt.* **1999**, *38*, 6337−6342.
(32) English, D. S.; Furube, A.; Barbara, P. F. *Chem. Phys. Lett.* **2000**, *324*, 15−19.
(33) Geddes, C. D.; Birch, D. J. S. *J. Non-Cryst. Solids* **2000**, *270*, 191−204.
(34) Wang, R.; Geiger, C.; Chen, L.; Swanson, B. *J. Am. Chem. Soc.* **2000**, *122*, 2399−2400.
(35) Wang, H. M.; Bardo, A. M.; Collinson, M. M.; Higgins, D. A. *J. Phys. Chem. B* **1998**, *102*, 7231−7237.
(36) Bardo, A. M.; Collinson, M. M.; Higgins, D. A. *Chem. Mater.* **2001**, *13*, 2713−2721.
(37) Xie, X. S.; Trautman, J. K. *Annu. Rev. Phys. Chem.* **1998**, *49*, 441−480.
(38) Moerner, W. E.; Orrit, M. *Science* **1999**, *283*, 1670−1676.
(39) Gimzewski, J. K.; Joachim, C. *Science* **1999**, *283*, 1683−1688.
(40) Mehta, A. D.; Rief, M.; Spudich, J. A.; Smith, D. A.; Simmons, R. M. *Science* **1999**, *283*, 1689−1695.
(41) Weiss, S. *Science* **1999**, *283*, 1676−1683.

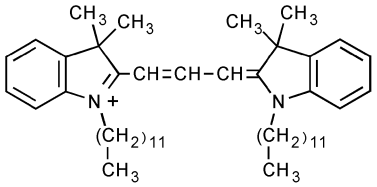

Figure 1. Molecular structure of DiI.

immediate surroundings. A better understanding of how an encapsulated molecule interacts with its local environment is therefore essential for the rational design of new photonic materials. This paper describes the single molecule spectroscopy of 1,1′-didodecyl-3,3,3′,3′-tetramethylindocarbocyanine (DiI) encapsulated in thin silica sol−gel films. We combine single molecule spectroscopy with fluorescence polarization detection to examine the correlation between the mobility and photostability of DiI encapsulated in the heterogeneous sol−gel silicate environment. Figure 1 illustrates the molecular structure of DiI.

Experimental Section

Materials. 99.9+% Tetraethyl orthosilicate (TEOS), spectrophotometric grade 95% ethanol, and 85 wt % phosphoric acid were purchased from Sigma-Aldrich. DiI was purchased from Molecular Probes. All chemicals were used without further purification. A phosphorous acid solution was prepared by diluting the 85 wt % stock solution 100 times using double-distilled water. Microscope cover glasses (Fisher Premium) were purchased from Fisher Scientific and were thoroughly cleaned before used.

Preparation of Sol Solution. TEOS sol solution was made from the acid hydrolysis of TEOS in an ethanol−water solution mixture in 1:8:7 molar ratios.[35,42] TEOS (177 μL) was first mixed with ethanol (358 μL), double-distilled water (100 μL), and the diluted phosphorous acid solution (2.0 μL). To facilitate hydrolysis, the solution mixture was sonicated for 2 h, during which time the temperature of the sonication bath was kept at 25 °C in order to minimize polycondensation. After sonication, the sol solution was slightly doped to 1.7 nM final dye concentration with a concentrated solution of DiI in ethanol. The DiI-doped sol solution was then allowed to age at ambient temperature in the dark for 24 h before it was used for thin silica sol−gel films preparation.

Casting of Sol−Gel Silicate Thin Films. Microscope cover glasses were used as the substrate for film casting. The cover glasses were cleaned by sonicating sequentially in 10% NaOH, acetone, and double-distilled water each for 20 min before used. To produce a thin sol−gel film for single molecule measurement, the aged DiI-doped sol solution (100 μL) was spin cast onto a cleaned cover glass at 6100 rpm for 70 s. The thickness of the film was determined by AFM to be 363 ± 20 nm. The sol−gel silicate films were allowed to age for three more days at ambient temperature in the dark before they were ready for single molecule measurement.

Single Molecule Spectroscopy. Fluorescence images of single DiI molecules were acquired by a home-built sample-scanning confocal microscope, which was based on an inverted microscope (Nikon, TE-200) and a nanopositioning stage equipped with position feedback electronics (Melles Griot, NanoBlock). Fluorescence images and kinetics traces from single DiI molecules were obtained under a continuous laser excitation at 543.5 nm, which is close to the λ_{max} of DiI encapsulated in a silica sol−gel monolith (551 nm), as illustrated in Figure 2. The laser excitation was delivered to the epi-illumination port of the microscope by a single-mode optical fiber, which also served as a 3.3 μm diameter spatial filter. The excitation laser that came out from the other end of the fiber was first collimated by a 10× objective,

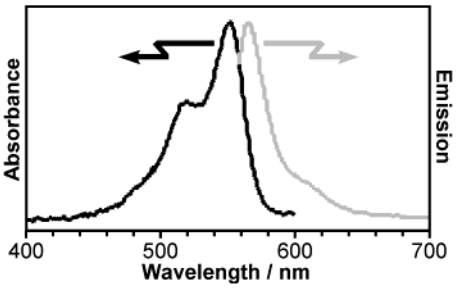

Figure 2. Absorption and emission spectra of DiI encapsulated in a sol−gel monolith. The emission spectrum was obtained from excitation at 551 nm.

filtered through a 543.5 nm interference filter, and then reflected up to a 100× microscope objective (Nikon, CFI Achromat oil immersion 1.25 N.A.) by a dichroic beam splitter (Chroma Technology). Fluorescence from single molecules collected by the same microscope objective was directed to exit from the side port of the microscope and clear a 100 μm aperture positioned at the first image plane. Fluorescence diverging from the aperture was then collimated with an achromatic lens and passed through a long-pass filter (Omega Optical, ALPHA Technology) to eliminate scattered laser excitation before it was directed to a polarizing beam splitter cube. The beam splitter cube resolved the fluorescence into a parallel ($I_{||}$) and a perpendicular ($I_{\perp}$) polarization component that were subsequently detected by two separate avalanche photodiode (APD) detectors (Perkin-Elmer, SPCM-AQR).

Upon raster scanning of a sol−gel silicate sample, each APD detector would produce a fluorescence image from the same sample area with the respective fluorescence polarization. The spot sizes of DiI molecules in the images were mostly diffraction limited and were measured at ∼280 nm. The typical size of a fluorescence image was fixed at 10 μm × 10 μm. To examine the photophysical properties of single molecules, a molecule was first chosen from a fluorescence image and then transported to the laser focus by the nanopositioning stage. The fluorescence kinetics trace of the chosen molecule could be collected by directing the collimated fluorescence to two separate APDs, where $I_{||}(t)$ and $I_{\perp}(t)$ were simultaneously monitored by the APDs at a 50 ms dwell time upon continuous laser excitation. On the other hand, the emission spectrum of the molecule could be acquired by directing the collimated fluorescence to a polychromator (Acton, SpectraPro 150) equipped with a liquid-nitrogen cooled CCD camera (Roper Scientific, SpectruMM). To prevent the transmission profile of the dichroic beam splitter from clipping the short wavelength portion of the emission spectrum, single DiI molecules were excited at 514.5 nm, which is near to the first vibronic band of the molecule.

Polarization Measurements and Mobility Classification. To measure the fluorescence polarization of single DiI molecules, the linearly polarized laser excitation was first converted to a circularly polarized excitation with a 543.5 nm $^1/_4$ waveplate before it was coupled into the single-mode optical fiber. The use of a circularly polarized excitation ensures that the random orientation of single molecules parallel to the sample plane does not affect the excitation efficiency of each molecule. From the $I_{||}(t)$ and $I_{\perp}(t)$ fluorescence kinetics traces, the polarization ($P(t)$) of fluorescence from single DiI molecules were calculated at all time according to

$$P(t) = \frac{I_{||}(t) - I_{\perp}(t)}{I_{||}(t) + I_{\perp}(t)} \quad (1)$$

In addition to the time-dependent polarization $P(t)$, an average polarization ($\bar{P}$) together with its standard deviation (σ_P) was also calculated as the statistical average of $P(t)$. To correct for the accumulated birefringence from various optical components as well as the different sensitivities of the two APDs, $\bar{P}$ values calculated from single molecules were always compared with the $\bar{P}$ of a concentrated DiI solution measured on the same day. Using the $\bar{P}$ determined from

(42) Mei, E.; Bardo, A. M.; Collinson, M. M.; Higgins, D. A. *J. Phys. Chem. B* **2000**, *104*, 9973−9980.

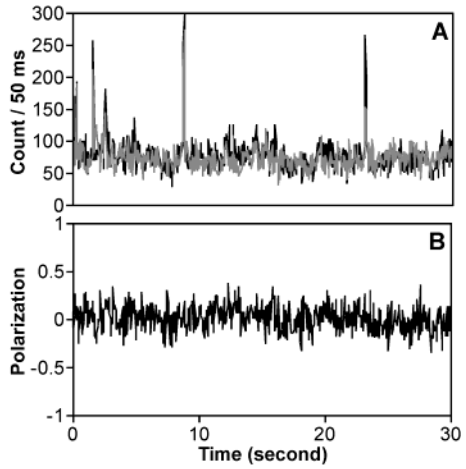

Figure 3. (A) $I_{||}(t)$ (black) and $I_{\perp}(t)$ (gray) collected from a DiI in ethanol solution. (B) The polarization plot ($P(t)$) calculated from $I_{||}(t)$ and $I_{\perp}(t)$ using eq 1.

the concentrated DiI solution as a reference for isotropic fluorescence, a DiI molecule could be assigned as "tumbling" or "fixed" accordingly.

Results and Discussions

Polarization of DiI Solution. The polarization of DiI in ethanol was determined from a 3.14 μM DiI in ethanol solution. Figure 3A shows the $I_{||}(t)$ and $I_{\perp}(t)$ measured from the solution together with the calculated $P(t)$ in Figure 3B. It is fairly apparent that the signals from the two channels are not quite identical, with $I_{||}$ usually larger than $I_{\perp}$, indicating the biased response from the $I_{||}$ and $I_{\perp}$ detecting channels. This bias most likely resulted from the birefringence of various optical components plus any difference in the sensitivity of the two APD detectors. Assuming that the emission from a solution is isotropic, we applied a scaling factor to $I_{||}(t)$ such that the calculated $\bar{P}$ of the solution was forced to zero. The same scaling factor would then be applied to all subsequent measurements of $I_{||}(t)$ performed on the same day in order to eliminate any systematic error introduced by the instrument when calculating the fluorescence polarization of single molecules. In addition to the scaling factor, the standard deviation of the properly scaled $\bar{P}$ of the concentrated DiI solution (σ_{iso}) was also calculated and subsequently used for the mobility classification of single DiI molecules. In our scheme, when the $\bar{P}$ of a single molecule is not within $\pm\sigma_{iso}$ from zero polarization, the molecule will be classified as fixed.

Identification of Single DiI Molecules. A 363 nm thick silica sol−gel film prepared from a 1.7 nM dye-doped sol solution should contain approximately 37 molecules per fluorescence image area of 10 μm × 10 μm. Figure 4 shows a fluorescence image of DiI encapsulated in a sol−gel silicate film. It is a 100 pixel × 100 pixel image with each pixel representing a physical area of 100 nm × 100 nm. The signal at each pixel was integrated for 50 ms, and the typical background count rate was less than 10 counts. Many diffraction-limited fluorescence spots can be identified from the image with the number density agreeing reasonably well with the calculated number density. The emission spectrum shown in Figure 4B confirms that the fluorescence was indeed originated from DiI molecules. Single molecule emission from a majority of the fluorescence spots in the image was confirmed by their corresponding kinetics traces, where an abrupt drop of fluorescence intensity down to the

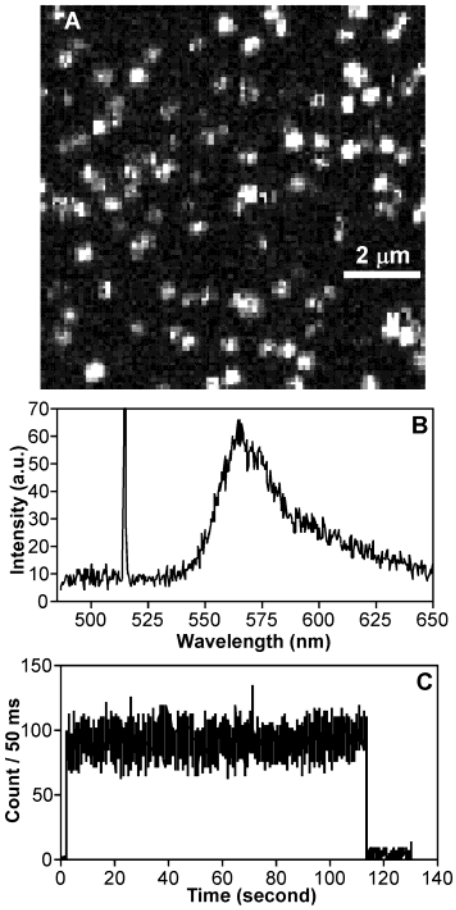

Figure 4. (A) Fluorescence image of DiI in a sol−gel silicate film. (B) The emission spectrum of a single DiI molecule when excited at 514.5 nm. (C) The fluorescence kinetics trace of a single DiI molecule.

background level was observed as a result of photobleaching (Figure 4C).

Single Molecule Studies of Silica Sol−Gel Films. The kinetics traces shown in Figure 5 exemplify the dynamic behavior displayed by DiI when it is encapsulated in sol−gel silicate. Unlike in polymer films, where the photophysics of DiI can mostly be described by a three-level system with negligible influence from guest−host interactions,[43,44] DiI in sol−gel silicate exhibits a much different behavior that is due to very rich dynamic interactions with its immediate surroundings. The observed intensity fluctuations in each kinetics trace are bigger than random shot noises, indicative of a second kind of dynamics occurring at a much faster time scale. Similar behavior has also been reported for rhodamine B and Nile Red encapsulated in silica sol−gel films.[36,42] In the case of rhodamine B, the intensity fluctuations were attributed to changes in the fluorescence quantum yield of the dye molecule because of rapid fluctuations in the environmental conditions.[42] It is highly probable that the same is happening to DiI when it is trapped inside a silica sol−gel film. Nevertheless, regardless of the exact origin of the intensity fluctuations, the survival time of each DiI molecule can still be accurately determined from the corresponding kinetics trace before the molecule is photobleached. The photostability of each molecule can then be directly inferred from the survival time measured.

(43) Trautman, J. K. *Proc. Robert A. Welch Found. Conf. Chem. Res.* **1995**, 173−181.

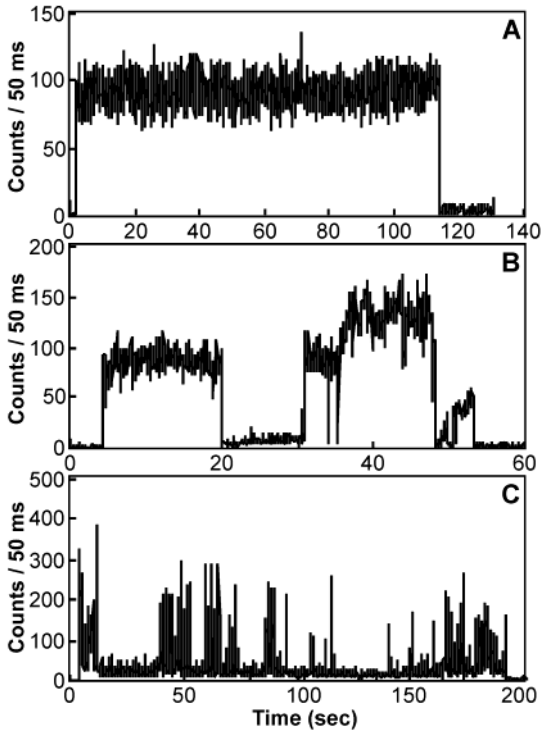

Figure 5. Examples of fluorescence trace from single DiI molecules with (A) single-level, (B) multilevel, and (C) multilevel-erratic transitions.

(i) Single Molecule Mobility. To determine if molecular motions contribute to the very rich dynamics observed, fluorescence polarization from single DiI molecules was measured using circularly polarized laser excitation. Figure 6 displays three fluorescence kinetics traces and the corresponding $P(t)$ plots that are related to different kinds of mobility observed from silica sol−gel encapsulated DiI molecules. The $P(t)$ plot in Figure 6A suggests that the molecule exhibits a fairly constant fluorescence polarization over time with $\bar{P} = 0.022 \pm 0.193$. The very small $\bar{P}$ indicates that the molecule is emitting isotropic fluorescence. This is possible if the molecule is free to tumble within its microcavity. Such behavior would be consistent with the notion that the molecule remains solvated at the interior of a pore that is filled with ethanol−water.[24] About 48% of the molecules from the aged 4-day old sample were found to exhibit such behavior. The molecule in Figure 6B also displays a fairly constant fluorescence polarization. Unlike the previous one, however, the fluorescence polarization of this molecule stays at -0.672 ± 0.065, which deviates substantially from zero. Accordingly, the molecule was assigned as a fixed molecule, suggesting that the molecule may be adhered to a pore wall, entrapped in a very small pore that prohibits rotation, or even buried deep inside a cleft such that the molecular motion is completely restrained.[24] When fluorescence dyes are used as tracers for undergroundwater studies, it is known that adsorptions of dye on mineral surfaces due to electrostatic interactions have a negative impact on the accuracy of hydrodynamic dispersion measurements.[45−47] The same argument may apply to sol−gel silicate at neutral pH, where the negatively charged surface tends to attract cationic dye molecules. Since DiI is a cationic dye, it is therefore possible that surface adsorptions due to electrostatic interactions may contribute significantly to the immobilization of DiI inside the sol−gel silicates thin films that we studied. On the other hand, electrostatic interactions may turn out to be irrelevant to the current investigation as the sol−gel films are prepared via the acidic hydrolysis of TEOS, leaving very few anionic sites available for electrostatic interactions inside the acidic sol−gel framework. Whether electrostatic interactions are responsible for the surface immobilization of most guest molecules inside sol−gel silicates is currently being investigated by comparing the polarization distributions of cationic rhodamine 6G and anionic sulforhodamine B molecules in sol−gel silicates. The results of this investigation will be reported elsewhere.[48]

Occasionally, a molecule may behave as neither tumbling nor fixed but a combination of both. In Figure 6C, we show a molecule that oscillates many times between tumbling and various fixed orientations. This behavior is clearly distinguished from the $P(t)$ plot, where the fluorescence polarization of this molecule is shown to vary considerably throughout the entire investigation. The $\bar{P}$ of this molecule was determined to be -0.243 ± 0.307. The substantial amount of uncertainty accompanying $\bar{P}$ reflects the dramatic variation in the fluorescence polarization of the molecule because of continuous molecular reorientation. Such kind of behavior would be consistent with a molecule that is locating at the solid−liquid interface. For instances, the molecule may adhere to the silica surface when it collides with the silica sol−gel framework, whereas the molecule may tumble freely when it is swept away from the surface.[24]

It is worth mentioning that the rapid intensity fluctuations associated with the fluorescence kinetics traces of these three types of molecules are quite comparable to each other, indicating that reorientation of the entire molecule within the silica sol−gel framework does not contribute significantly to the observed intensity fluctuations. In addition, Figure 6C also suggests that the time scale of molecular reorientation for those oscillating molecules is much longer than the time scale of the rapid intensity fluctuations. This further eliminates molecular motion as a potential source of intensity fluctuations. Exactly what causes the rapid intensity fluctuations will be a subject of future investigations.[42]

In Figure 7, we present the distribution of $\bar{P}$ determined from a total of 212 single DiI molecules. Because of the depolarization effect of a high N.A. microscope objective, a randomly oriented emission dipole with component (x,y,z) will contribute to $I_{||}$ and $I_{\perp}$, according to the following equations.[49,50]

$$I_{||} = I_{tot}(K_1x^2 + K_2y^2 + K_3z^2) \quad (2a)$$

$$I_{\perp} = I_{tot}(K_2x^2 + K_1y^2 + K_3z^2) \quad (2b)$$

Where the optical axis of the objective is parallel to the z-axis, I_{tot} is the total emission intensity,

$$K_1 = {}^3/_{32}(5 - 3\cos\theta_{obj} - \cos^2\theta_{obj} - \cos^3\theta_{obj}) \quad (2c)$$

$$K_2 = {}^1/_{32}(1 - 3\cos\theta_{obj} + \cos^2\theta_{obj} - \cos^3\theta_{obj}) \quad (2d)$$

$$K_3 = {}^1/_{8}(2 - 3\cos\theta_{obj} + \cos^3\theta_{obj}) \quad (2e)$$

$$\text{N.A.} = n\sin\theta_{obj} \quad (2f)$$

(44) Yip, W. T.; Hu, D. H.; Yu, J.; Vandenbout, D. A.; Barbara, P. F. *J. Phys. Chem. A* **1998**, *102*, 7564−7575.
(45) Kasnavia, T.; Vu, D.; Sabatini, D. A. *Ground Water* **1999**, *37*, 376−381.
(46) Sabatini, D. A. *Ground Water* **2000**, *38*, 651−656.
(47) Ray, K.; Nakahara, H. *J. Phys. Chem. B* **2002**, *106*, 92−100.

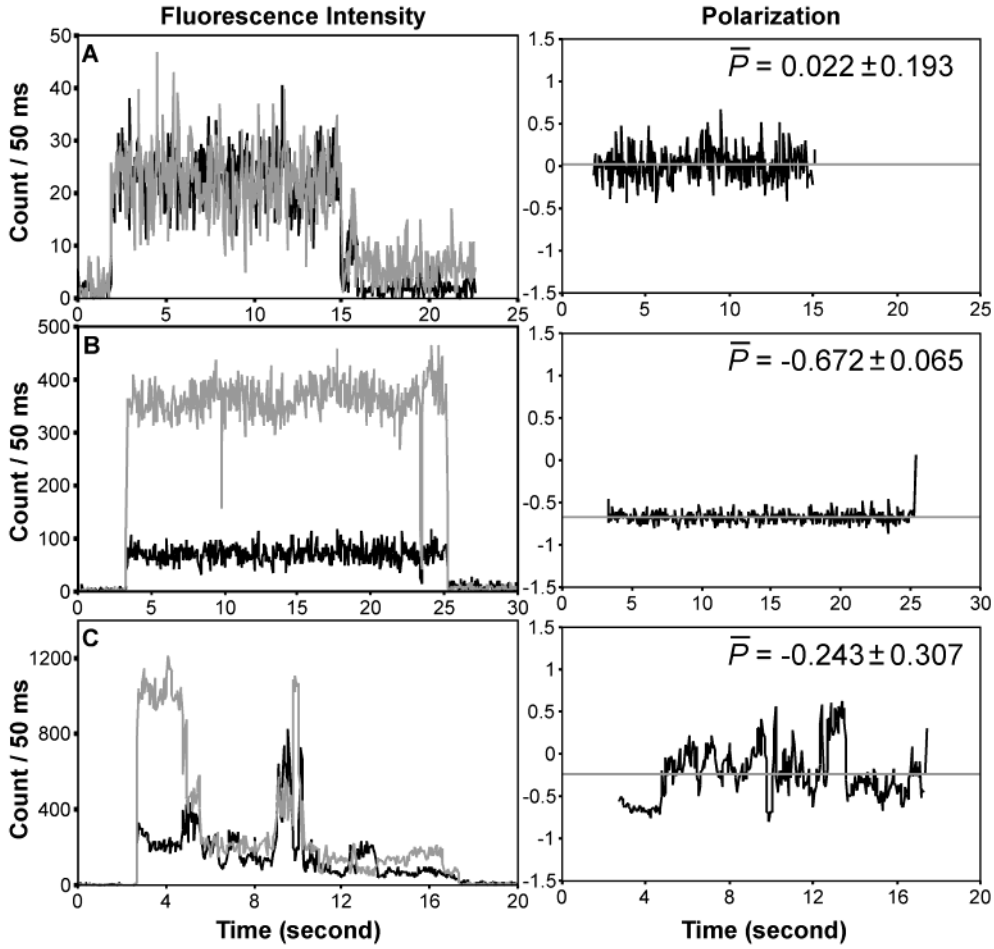

Figure 6. Fluorescence intensity and polarization of three single DiI molecules that display three different behaviors. (A) A molecule that tumbles freely with an average polarization close to zero. (B) A molecule that is completely immobilized with an average polarization equals −0.672. (C) A molecule that switches between tumbling and immobilized or between different orientations. Black and gray lines in the fluorescence traces represent $I_{\parallel}(t)$ and $I_{\perp}(t)$, respectively. The gray line in the polarization plot indicates the average polarization ($\bar{P}$) of the molecule.

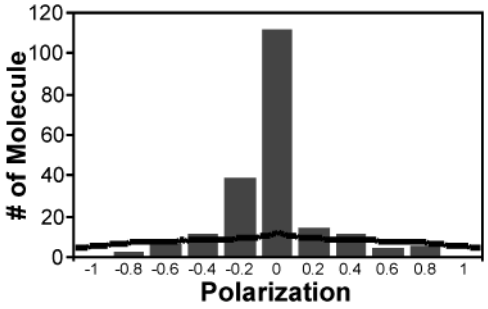

Figure 7. Histogram of $\bar{P}$. The solid line represents a theoretical fit that is based on applying eq 3 to a collection of fixed DiI molecules randomly oriented throughout the entire silica sol−gel framework.

Substituting $I_{\parallel}$ and $I_{\perp}$ in eq 1 with eqs 2a and 2b gives the polarization of the emission dipole as

$$P = \frac{(K_1 - K_2)(x^2 - y^2)}{(K_1 + K_2)(x^2 + y^2) + 2K_3z^2} \qquad (3)$$

When N.A. is low, $K_1 \gg K_2$ and K_3, reducing eq 3 directly back to eq 1. When N.A. is high, K_2 and K_3 are no longer negligible and the polarization distribution of a collection of randomly oriented emission dipoles will skew toward zero polarization, creating a peak at the center of the distribution[51] instead of a trough that would have been predicted by eq 1 alone. For a 1.25 N.A. oil immersion microscope objective, $n = 1.52$, $\theta_{obj} = 55.32°$, $K_1 = 0.2611$, $K_2 = 0.0025$, and $K_3 = 0.0597$. The histogram in Figure 7 clearly suggests that the distribution of $\bar{P}$ does not conform to a collection of fixed DiI molecules that are randomly oriented inside a sol−gel silicate film. In fact, the very poor fit at $\bar{P}$ around zero suggests that there are more molecules exhibiting zero polarization than the depolarization effect can account for. This is a very strong indication that, in addition to fixed molecules, the sample also contains a lot of tumbling molecules, which give off isotropic fluorescence and thereby producing zero fluorescence polarization. There are altogether 101 tumbling molecules found, which account for 48% of the total number of DiI molecules we investigated. It is worth mentioning that, according to the theoretical fit, there will be about 12 fixed molecules mistakenly assigned to the group of 101 tumbling molecules. These 12% incorrectly assigned molecules have the projection of their emission dipoles on the $x-y$ plane making an angle about 45° from the x-axis,

(48) Manuscript in preparation.
(49) Axelrod, D. *Biophys. J.* **1979**, *26*, 557−573.
(50) Ha, T.; Laurence, T. A.; Chemla, D. S.; Weiss, S. *J. Phys. Chem. B* **1999**, *103*, 6839−6850.
(51) Garcia-Parajo, M. F.; Koopman, M.; van Dijk, E.; Subramaniam, V.; van Hulst, N. F. *Proc. Natl. Acad. Sci. U.S.A.* **2001**, *98*, 14392−14397.

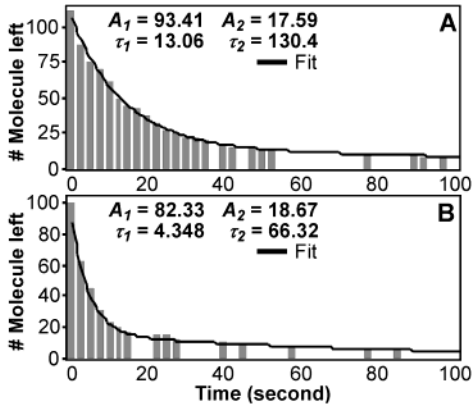

Figure 8. Survival histograms of single DiI molecules upon continuous excitation at 543.5 nm. (A) Fixed and (B) tumbling molecules. Both histograms are fitted with a biexponential decay function with the number of molecule left = $A_1 \exp(-t/\tau_1) + A_2 \exp(-t/\tau_2)$.

rendering the measured polarization zero that eventually leads to the erroneous assignments.

(ii) Correlation Between Mobility and Photostability. Using the above technique, most single DiI molecules could be classified into two groups, namely "tumbling" and "fixed" molecules, with a different emphasis on the nature of their local environments, respectively. With this scheme, the effect of the local environment on the optical properties of silica sol−gel encapsulated DiI could be examined. For example, from the same set of fluorescence kinetics trace data, we could simultaneously classify the mobility and measure the photostability of every single DiI molecule. We compare in Figure 8 the histograms constructed from the photostability of the fixed and tumbling DiI molecules encapsulated in silica sol−gel films. Both histograms display biexponential decay kinetics, signifying further the heterogeneous nature of the silica sol−gel environment experienced by the molecules in each subgroup.

For the group of fixed molecules, it was expected that their optical properties would be extremely sensitive to the associated guest−host interactions, which depend critically on the nature of the point of contact upon DiI immobilization on a sol−gel silicate framework. While such kind of interactions should be highly heterogeneous, it is rather amazing to see that a biexponential decay function is sufficient to describe the photostability of the fixed molecules ($R^2 = 0.995$). Apparently, there are only a limited number of parameters that control the photostability of a fixed molecule despite the heterogeneity of its local environment. Figure 8A suggests that the survival lifetime of the majority (84%) of the 111 fixed molecules is 13.1 s. The remaining 16% of the fixed molecules exhibit a substantially higher photostability, with a survival lifetime approaching 130 s.

On the contrary, while one may expect that the photostability of the free DiI molecules would resemble DiI dissolved in ethanol and display a single exponential decay, it is truly surprising to see that a biexponential fit is required to describe the photostability of the free molecules shown in Figure 8B ($R^2 = 0.998$). Out of a total of 101 free molecules, 82 display a survival lifetime of 4.3 s. This relatively short survival lifetime accounts for 81% of the free molecules studied, with the remaining 19% exhibiting a longer survival lifetime of 66.3 s. It is unlikely that the longer-lived molecules in the biexponential decay are due to the presence of the erroneously assigned fixed molecules, as they constitute 19% of the total population instead of the 12% predicted by theory. Moreover, the survival lifetime of the majority of the fixed molecules is more than four times shorter than 66.3 s, making them an even less likely candidate for the observed longer lived molecules. It is therefore quite possible that some pores in the silica sol−gel film may be just big enough for a fully solvated molecule to tumble yet too small to leave the solvent shell of the molecule unperturbed while it is tumbling.[24,52−54] As a result, the optical properties of the free DiI may be quite different from those found in a DiI solution. At this point, the temporal resolution (50 ms) of our instrument is insufficient to distinguish the difference between hindered and truly free motions in single molecules. It is believed that time-resolved single molecule anisotropy measurements should provide additional insight into the optical properties and the nature of the local environment of this group of molecules.[55,56]

According to the histograms shown in Figure 8, our measurements suggest that the photostability of both the major and minor components of the fixed molecules is higher than the respective components of the free molecules. In particular, when only the major components are considered, our studies further indicate that the photostability of the fixed molecules is three times higher than the free molecules. This result is qualitatively consistent with previous studies on sol−gel monoliths, where an encapsulated dye usually exhibits enhanced photostability.[15,25,26] More importantly, this work establishes a direct correlation between the mobility and photostability of sol−gel encapsulated dye molecules. This level of microscopic information was previously unavailable in ensemble measurements. In addition, our enhancement factor is in remarkable agreement with the observed 4-fold increase in photostability exhibited by rhodamine B in dried silicate thin films relative to those in wet samples.[42] It is therefore very likely that when a film is dried and the solution content is completely vaporized, the dye dopants will be left immobilized on the surface of a silica sol−gel framework. Immobilization leads to the reduction of intramolecular motions, thereby reducing the number of dynamic interactions that lead to photodegradation, hence increasing photostability.

The suppression of oxygen diffusion probably plays an insignificant role in the observed improvement in photostability, since the thickness of our samples is only 363 ± 20 nm. On the other hand, the very high photostability displayed by the minor fraction (16%) of the fixed molecules is most likely due to a few molecules buried deep inside narrow clefts that are extremely difficult for oxygen gas to reach.

Conclusions

Using DiI as a fluorescence probe, the physical and optical properties of a silica sol−gel encapsulated guest molecule have been investigated with single molecule spectroscopy. Because of the capability of single molecule spectroscopy to decipher heterogeneous dynamics, this work has provided valuable insight

(52) Zheng, L. L.; Reid, W. R.; Brennan, J. D. *Anal. Chem.* **1997**, *69*, 3940−3949.
(53) Gottfried, D. S.; Kagan, A.; Hoffman, B. M.; Friedman, J. M. *J. Phys. Chem. B* **1999**, *103*, 2803−2807.
(54) Geddes, C. D.; Karolin, J.; Birch, D. J. S. *J. Phys. Chem. B* **2002**, *106*, 3835−3841.
(55) Harms, G. S.; Sonnleitner, M.; Schutz, G. J.; Gruber, H. J.; Schmidt, T. *Biophys. J.* **1999**, *77*, 2864−2870.
(56) Schaffer, J.; Volkmer, A.; Eggeling, C.; Subramaniam, V.; Striker, G.; Seidel, C. A. M. *J. Phys. Chem. A* **1999**, *103*, 331−336.

into both the structural and chemical heterogeneity of the silica sol−gel environment. In this study, the mobility of single DiI molecules has been readily classified into tumbling and fixed, according to their respective fluorescence polarizations. The ability to separate the guest molecules into different subgroups provides a unique opportunity to examine the effect of guest−host interactions on the physical, chemical, and optical properties of each subgroup of guest molecules that are entrapped inside very different local environments. Such kind of microscopic information is critical to the rational design and fabrication of new photonic devices as well as sol−gel derived sensors and catalyst materials. Using single molecule spectroscopy to measure the mobility and photostability of silica sol−gel encapsulated DiI molecules simultaneously, the relationship between mobility and photostability has been established. It was found that DiI experiences a 3-fold increase in photostability upon immobilization, demonstrating unequivocally that hindered intramolecular motions do lead to higher photostability. It is expected that the application of this same technique to the study of other molecular properties as a function of mobility should yield further insight to the nature of the local environment surrounding a guest molecule and provide a better assessment on the impact of environmental heterogeneity on guest−host interactions within sol−gel derived materials. Finally, the very slow reorientation rate displayed by some DiI molecules that oscillate between tumbling and fixed also suggests that reorientation of the entire guest molecule does not have a significant contribution to the rapid intensity fluctuations observed in the fluorescence kinetics trace of single DiI molecules. The exact origin of the intensity fluctuations has yet to be determined.

Acknowledgment. W.T.Y. acknowledges Professor Matthew B. Johnson for performing the AFM measurement. This work was supported by the University of Oklahoma (startup funds) and the Petroleum Research Fund administered by the American Chemical Society.

JA026533K